Nonadiabatic transitions in finite-time adiabatic rapid passage

T. Lu,[1] X. Miao,[2] and H. Metcalf[2]

[1]*Computational Science Center, Brookhaven National Laboratory, Upton, New York 11973, USA*
[2]*Physics and Astronomy, Stony Brook University, Stony Brook, New York 11794-3800, USA*

To apply the adiabatic rapid passage process repetitively [T. Lu, X. Miao, and H. Metcalf, Phys. Rev. A **71**, 061405(R) (2005)], the nonadiabatic transition probability of a two-level atom subject to chirped light pulses over a finite period of time needs to be calculated. Using a unitary first-order perturbation method in the rotating adiabatic frame, an approximate formula has been derived for such transition probabilities in the entire parameter space of the pulses.

PACS number(s): 32.80.Pj, 42.50.Vk

I. BACKGROUND

Adiabatic rapid passage (ARP) is a long-studied method of inverting the population of a two-level system that has been well known since the early days of magnetic resonance. The population inversion occurs as the result of a very large frequency sweep through the resonance condition in a very long time, so the sweeps are typically approximated as infinite. By contrast, exploitation of ARP for producing large optical forces requires repeated sweeps of both the optical frequency and the amplitude of the light field so they are necessarily finite in both frequency range and duration. In either case the population inversion may be incomplete, and we denote the probability for not making the desired adiabatic transition as P_{nad}.

When the light beams are oppositely directed, a pair of appropriately timed (nonoverlapping) sweeps coherently exchanges momentum between them, imparting the difference $2\hbar k$ to the atoms. When these cycles are repeated at rate $\omega_m \gg \gamma$, the force is $F_{ARP} = \hbar k \omega_m / \pi \gg \hbar k \gamma / 2$, the usual radiative force on the atoms [1,2]. Here $\lambda = 2\pi/k$ is the wavelength of the transition to an excited state of lifetime $1/\gamma$. In this paper we show that the details of both frequency and amplitude sweep wave forms can have a dramatic impact on the parameter dependence of P_{nad}. If the counterpropagating light pulses overlap in time in the interaction region, the momentum exchange between each pair can exceed $2\hbar k$ due to multiphoton transitions [3]. However, this force is not directly related to P_{nad}, and it is beyond the scope of this paper.

Numerical calculations for repetitive sweeps [1] have shown that sinusoidal wave forms result in P_{nad} distributions that have desirable consequences with readily accessible parameters, and experiments confirm these results [2]. However, there are modest differences between the measurements and the calculations, and these may be partially attributed to sweep wave forms that are not precisely sinusoidal. To explore this, we have recalculated the ARP map of Ref. [1] with different wave forms, and have found very significant qualitative differences among the results. In addition, we have developed an analytic approximation for P_{nad} that is appropriate for a large class of finite wave forms.

We consider the reference frame that rotates at the frequency of the light field so that the Hamiltonian $\mathcal{H}_R$ can be written as [4]

$$\mathcal{H}_R(t) = \frac{\hbar}{2} \begin{pmatrix} \delta(t) & \Omega(t) \\ \Omega(t) & -\delta(t) \end{pmatrix}, \qquad (1)$$

where $\delta \equiv \omega_\ell - \omega_a$ is the detuning of the light at frequency ω_ℓ from the atomic resonance at ω_a, and $\Omega \equiv e\langle g|\vec{E}\cdot\vec{r}|e\rangle/\hbar$ is the Rabi frequency that characterizes the on-resonance, electric dipole interaction between the light and atoms. The ARP process can be envisioned in a dressed-atom view of the energies of the two-level system (see Refs. [1,5]). An alternative view is the rotation of the Bloch vector $\vec{R}(t) = \langle\psi(t)|\vec{\sigma}|\psi(t)\rangle$, where the $\vec{\sigma}$ is an artificial vector whose components are the Pauli matrices, on the Bloch sphere under the influence of the modulated light field. The vertical axis (z) of the sphere is the population difference term and the horizontal axes are related to the relative phase of the atomic superposition (see Ref. [4]). The equation of motion, $d\vec{R}/dt = \vec{\Omega}(t) \times \vec{R}$, can be derived from Eq. (1). Here $\vec{\Omega}(t)$ is an artificial "torque" vector having components $[\Omega(t), 0, \delta(t)]$.

The process of ARP in this view involves a synchronized sweep of both the amplitude and frequency of the light so that the torque vector sweeps along a meridian from one pole to the other. As illustrated in Fig. 1(a), if the initial state lies
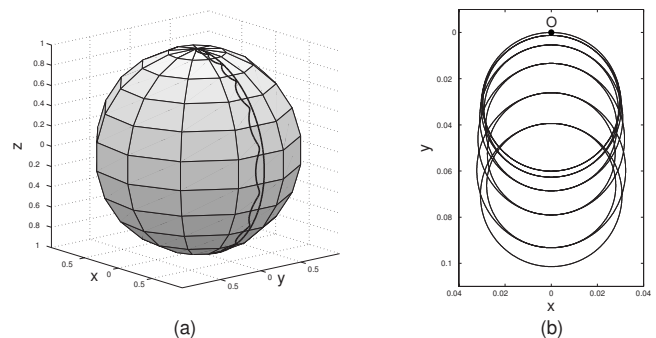

FIG. 1. Adiabatic following of the Bloch vector along the track of the torque vector of a modulated light pulse. (a) The wavy curve connecting two poles is a typical trace of the Bloch vector on the Bloch sphere. The meridian close to it is the trace of the torque vector. (b) The same pair of traces in the adiabatic frame. The meridian reduces to a fixed point at origin in the adiabatic frame.
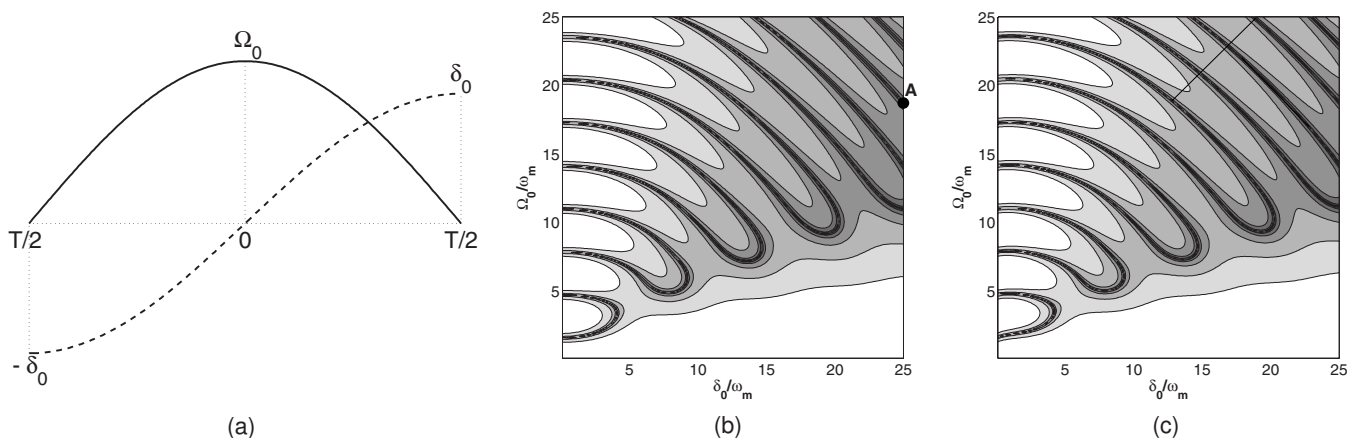
FIG. 2. Contour map of P_{nad} for sinusoidal pulses. (a) The profiles of the pulse detuning and Rabi frequency. (b) The contour curves of $P_{nad}=0.1, 0.01, \ldots$. The darkest regions represent zeros of P_{nad}. The point A with coordinates [25, 18.724] in part (b) corresponds to the trace of Bloch vector shown in Fig. 1. (c) The contour plot of the approximate P_{nad}.

in an eigenstate, $\vec{R}$ will start from a pole and precess around the torque vector to the other pole. As long as the sweep is slow enough, the population will be completely inverted at the end. Figure 1(b) shows the trace of the Bloch vector in the adiabatic frame. The adiabatic frame rotates together with the torque vector along the meridian (but without precession), so that the torque vector is fixed at the origin, which is point O in Fig. 1(b), while the Bloch vector starts from and ends at the same point O over the duration of a pulse.

If the sweep is not slow enough, the Bloch vector does not follow the torque vector adiabatically, and there is a small fraction of the population not inverted at the end of each sweep. The amount of the small fraction is called the nonadiabatic transition probability, denoted by P_{nad}. In order to design sweep schemes with vanishingly small P_{nad}, we need to calculate P_{nad} for various pulse schemes and parameters. The ARP process is usually used for one-time population inversions, where the sweep time can be regarded as infinite. Extensive research has been done in this area [6–10], while the focus of this paper is on the class of finite-time sweeps.

II. CHARACTERISTICS OF THE P_{nad} DISTRIBUTION

The value of P_{nad} resulting from a chirped light pulse depends on the maximum pulse intensity, denoted by Ω_0, the maximum detuning, denoted by δ_0, and the pulse profile. We start from a sinusoidally varying light pulse, whose time dependence is described by

$$\Omega(t) = \Omega_0 \cos \omega_m t, \quad \delta(t) = \delta_0 \sin \omega_m t, \quad (2)$$

where $\omega_m = \pi/T$ and $-T/2 \leq t \leq T/2$. The pulse profile is plotted in Fig. 2(a). The special case of $\Omega_0 = \delta_0$ has been studied analytically in some detail [11]. Assuming that the atom starts in the ground state, we integrate the Schrödinger equation numerically from $-T/2$ to $T/2$ and calculate the remaining ground state population at the end, which gives P_{nad} for the process. From dimensional analysis, P_{nad} is a function of two dimensionless parameters δ_0/ω_m and Ω_0/ω_m.

For the case of $\Omega_0 = \delta_0$, we reproduce the results of Ref. [11]. The two-dimensional map of P_{nad} is plotted in Fig. 2(b). The lower-left corner of Fig. 2(b) has been corroborated experimentally [2].

The P_{nad} map is divided into two regions—oscillatory and nonoscillatory. Just as pointed out in Ref. [10] for infinite-time transitions, each oscillation is connected to an integer number of precessions of the Bloch vector during the time evolution. For example, Fig. 1 shows the trace of the Bloch vector under the influence of a sinusoidal light pulse with parameters at point A in Fig. 2(b). Point A in Fig. 2(b) lies on the 11th curve counted from the origin along the diagonal. Correspondingly, Fig. 1(b) shows that in the adiabatic frame, the Bloch vector precesses exactly 11 cycles while the torque vector is fixed at the origin. Along each "loop" of zeros of P_{nad} [the darkest regions in Fig. 2(b)], there is a special point connecting the upper arc and lower arc, whose precession number differs by one.

Roughly speaking, in the nonoscillatory region $\delta_0 \gg \Omega_0$, the nonadiabatic transition is dominated by the barely avoided crossing at resonance, and the Landau-Zener formula applies,

$$P_{nad} \sim \exp\left(-\frac{\pi}{2}\frac{\Omega_0^2}{\dot{\delta}_0}\right) = \exp\left(-\frac{\pi}{2}\frac{\Omega_0^2}{\delta_0 \omega_m}\right). \quad (3)$$

In the oscillatory region, the oscillation amplitude of P_{nad} decreases from 1 to 0 as δ_0/Ω_0 increases. For an unchirped pulse, i.e., $\delta_0 = 0$,

$$P_{nad} = \cos^2\left(\int_0^{T/2} \Omega(t)dt\right) = \cos^2\left(\frac{\Omega_0}{\omega_m}\right). \quad (4)$$

It agrees with the area theorem [4]. To attain complete population inversion, i.e., $P_{nad} = 0$, with an unchirped pulse, the integral of the eigenfrequency $\Omega(t)$ over the entire pulse must be an *odd* multiple of π. In the adiabatic limit, i.e., $\Omega_0 \to \infty$ and $\delta_0 \to \infty$ simultaneously with their ratio fixed, or equivalently, $\hbar \to 0$, we will show later that
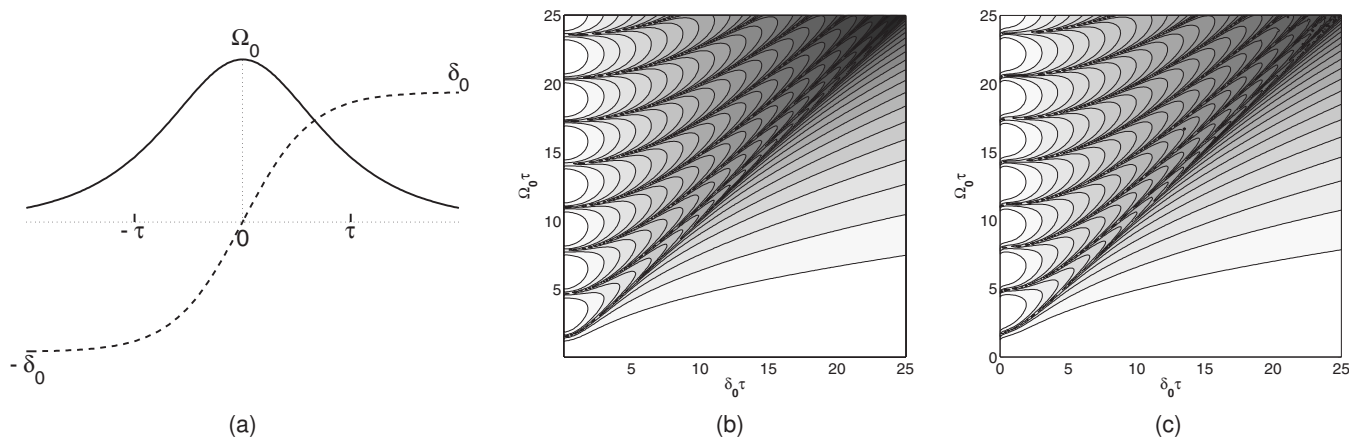
FIG. 3. Contour map of P_{nad} for the Demkov-Kunike model. (a) The profiles of the detuning and Rabi frequency. (b) The contour curves of $P_{nad}=0.1, 0.01, \ldots$. The darkest regions represent zeros of P_{nad}. (c) The contour plot of the approximate P_{nad}.

$$P_{nad} \sim \left(\frac{\delta_0^2}{\dot{\Omega}\left(\frac{T}{2}\right)} \right)^{-2} \sin^2\left(\int_0^{T/2} \Omega'(t)dt \right)$$

$$= \left(\frac{\delta_0^2}{\Omega_0 \omega_m} \right)^{-2} \sin^2\left(\int_0^{T/2} \Omega'(t)dt \right), \qquad (5)$$

where $\Omega'(t) = \sqrt{\delta^2(t) + \Omega^2(t)}$ is the generalized Rabi frequency. To attain complete population inversion in the adiabatic limit, the integral of the eigenfrequency $\Omega'(t)$ over the entire pulse must be an *integer* multiple of 2π. All characteristics of the P_{nad} map described above are true for general pulse profiles. Precise asymptotic forms of P_{nad} will be presented with detailed derivation in a forthcoming paper.

It is instructive to compare the P_{nad} map for finite-time sinusoidal pulses, which is not exactly solvable, to that for infinite-time pulses in the Demkov-Kunike (DK) model [7,10], which has a similar pulse profile but is exactly solvable. The time dependence of the field in the DK model is

$$\Omega(t) = \Omega_0 \operatorname{sech}\left(\frac{\pi t}{2\tau}\right), \quad \delta(t) = \delta_0 \tanh\left(\frac{\pi t}{2\tau}\right). \qquad (6)$$

The pulse profile of the DK model, which is plotted in Fig. 3(a), is similar to that of sinusoidal pulses except for the tails at large $|t|$. The special case of $\Omega_0^2 - \delta_0^2 = (\pi/2\tau)^2$ was studied in Ref. [4]. The nonadiabatic transition probability of the DK model was derived in Ref. [10],

$$P_{nad}^{DK} = \frac{\cosh^2 \tau\sqrt{\delta_0^2 - \Omega_0^2}}{\cosh^2 \tau\delta_0}. \qquad (7)$$

The contour map of P_{nad} for the DK model is plotted in Fig. 3(b). As in Fig. 2(b), it has a nonoscillatory region where the Landau-Zener formula applies; for unchirped pulses the area theorem also applies. However, the figures differ significantly in the oscillatory region because Eq. (5) does not agree with Eq. (7) in the adiabatic limit. As a conclusion, the seemingly negligible tails in the pulse profile makes a big difference in the map of P_{nad}. Equation (7) is a poor approximation of P_{nad} for sinusoidal pulses.

In the following section we will derive a simple formula that serves as a good approximation for P_{nad} of finite-time pulses in the entire map.

III. APPROXIMATE FORMULA FOR P_{nad}

We derive an approximate formula for P_{nad} for finite-time pulses with large intensity and detuning. It is obtained by a first order perturbation calculation in the appropriate reference frame. The rotating frame is not appropriate because the Hamiltonian in it [see Eq. (1)] is large and so the atomic state changes quickly. Since the atomic state follows the energy eigenstate adiabatically under such a pulse, the adiabatic frame is more appropriate. The transformation matrix from the rotating frame to the adiabatic frame is formed by instantaneous energy eigenstates, which are called the dressed states of the atom in the field [12],

$$U_A(t) = \begin{pmatrix} \cos(\theta/2) & \sin(\theta/2) \\ -\sin(\theta/2) & \cos(\theta/2) \end{pmatrix}, \qquad (8)$$

where $0 \leq \theta \leq \pi$ with $\tan\theta(t) = \Omega(t)/\delta(t)$. The Hamiltonian in the adiabatic frame is

$$\mathcal{H}_A(t) = U_A \mathcal{H}_R U_A^\dagger - i\hbar U_A \frac{d}{dt} U_A^\dagger = \frac{\hbar}{2} \begin{pmatrix} \Omega'(t) & i\dot{\theta}(t) \\ -i\dot{\theta}(t) & -\Omega'(t) \end{pmatrix}. \qquad (9)$$

The large diagonal elements of $\mathcal{H}_A$ indicate that the atomic state has a rapidly changing phase as it follows the energy eigenstate. In the Bloch sphere view, it means that the Bloch vector precesses rapidly around the torque vector. Only in a reference frame that rotates at the same frequency about the eigenstate (the torque vector) does the atomic state (the Bloch vector) change slowly enough so that a perturbation method can be applied. Such a frame is called the rotating (precessing) adiabatic frame [8,10]. The transformation matrix associated with the rotation is

$$U_R(t) = \begin{pmatrix} e^{is(t)/2} & 0 \\ 0 & e^{-is(t)/2} \end{pmatrix}, \tag{10}$$

where $s(t) = \int_0^t \Omega'(\tau) d\tau$. The Hamiltonian in the rotating adiabatic frame is

$$\mathcal{H}(t) = U_R \mathcal{H}_A U_R^\dagger - i\hbar U_R \frac{d}{dt} U_R^\dagger = \frac{\hbar}{2} \begin{pmatrix} 0 & i\dot{\theta}(t) e^{is(t)} \\ -i\dot{\theta}(t) e^{-is(t)} & 0 \end{pmatrix}. \tag{11}$$

The absolute value of $\mathcal{H}(t)$ is not small for highly detuned intense pulses, but due to the rapidly changing phase $s(t)$, the evolution of the atomic state in this frame is indeed slow. In general the Schrödinger equation in the rotating adiabatic frame is not exactly solvable. A formal solution can be written as the Dyson expansion that involves nested time integrations and time-ordered products [13,14].

Here we apply the perturbation method in the rotating adiabatic frame. Denote the propagation matrix for time from 0 to t by $O(t)$. The first order perturbation gives

$$O(t) \sim I - \frac{i}{\hbar} \int_0^t \mathcal{H}(\tau) d\tau. \tag{12}$$

However, this approximation is not unitary, which can lead to unphysical results if used repeatedly. A better option is to use

$$\hat{O}(t) = \exp\left(-\frac{i}{\hbar} \int_0^t \mathcal{H}(\tau) d\tau\right), \tag{13}$$

which is called the unitary first order approximation. Equation (13) ignores the noncommutativity between the Hamiltonians at different times, therefore it is exact only for commutative Hamiltonians. Nevertheless, as demonstrated below, Eq. (13) serves as a good approximation for the mapping of P_{nad} resulting from a general chirped light pulse. Substituting Eq. (11) into Eq. (13), we can obtain the explicit form of $\hat{O}(t)$,

$$\hat{O}(t) = \exp\left\{-i\begin{pmatrix} 0 & iz(t) \\ -iz^*(t) & 0 \end{pmatrix}\right\}$$
$$= \begin{pmatrix} \cos|z(t)| & \frac{z(t)}{|z(t)|} \sin|z(t)| \\ -\frac{z^*(t)}{|z(t)|} \sin|z(t)| & \cos|z(t)| \end{pmatrix}, \tag{14}$$

where $z(t) = \frac{1}{2} \int_0^t d\tau \dot{\theta}(\tau) e^{is(\tau)}$ and $z^*(t)$ is the complex conjugate of $z(t)$.

In spite of the unitarity, Eq. (13) is still only of first order accuracy. Higher order unitary approximations for $O(t)$ can also be derived from the Dyson expansion. However, their expressions and evaluations are more complicated and will not be discussed in this paper.

The nonadiabatic transition amplitude is the off-diagonal element of the propagation matrix in the rotating adiabatic frame for the entire pulse ($[-T/2, T/2]$). Successive application of the unitary approximation to the propagation matrix

on each half pulse ($[-T/2, 0]$ and $[0, T/2]$) enhances the accuracy of $\hat{O}$ for the entire pulse, from which $\hat{P}_{nad}$ is derived. For simplicity, we only consider symmetric pulses in this paper, i.e., $\delta(-t) = -\delta(t)$, $\Omega(-t) = \Omega(t)$. For such pulses the propagation matrices for the two half pulses are related in a simple way. Denote the propagation matrix $O(t)$ by

$$O(t) = \begin{pmatrix} \alpha^*(t) & -\beta(t) \\ \beta^*(t) & \alpha(t) \end{pmatrix}. \tag{15}$$

For a symmetric pulse we have

$$O_{[-T/2, T/2]} = O_{[0, T/2]} O_{[-T/2, 0]}$$
$$= \begin{pmatrix} \alpha^*(T/2) & -\beta(T/2) \\ \beta^*(T/2) & \alpha(T/2) \end{pmatrix} \begin{pmatrix} \alpha^*(T/2) & -\beta^*(T/2) \\ \beta(T/2) & \alpha(T/2) \end{pmatrix}. \tag{16}$$

So

$$P_{nad} = [\alpha(T/2)\beta(T/2) + \alpha^*(T/2)\beta^*(T/2)]^2. \tag{17}$$

Comparison between Eqs. (14) and (15) gives the approximation for $\alpha(t)$ and $\beta(t)$. Substituting the approximations $\hat{\alpha}(t)$ and $\hat{\beta}(t)$ into Eq. (17), we have the approximate formula for P_{nad},

$$\hat{P}_{nad} = \sin^2\left|\int_0^{T/2} dt\, \dot{\theta}(t) e^{is(t)}\right| \cos^2\left(\arg\int_0^{T/2} dt\, \dot{\theta}(t) e^{is(t)}\right). \tag{18}$$

The contour map of $\hat{P}_{nad}$ for sinusoidal pulses is plotted in Fig. 2(c). It is in good quantitative agreement with the contour map of the exact P_{nad} in Fig. 2(b). The maximum error is 0.176 at a point near origin. To demonstrate the universality of Eq. (18), we did the same comparison for triangular pulses. The time dependence of the intensity and the frequency sweep for a triangular pulse is

$$\Omega(t) = \Omega_0(1 - |2t/T|), \quad \delta(t) = \delta_0(2t/T). \tag{19}$$

The pulse profile is plotted in Fig. 4(a). In the Bloch sphere view of the problem, the torque vector moves along a straight line with uniform speed for each half pulse. The problem reduces to the Landau-Zener model in a rotated frame, and thus is solvable in terms of confluent geometric functions. The map of the exact P_{nad} is plotted in Fig. 4(b). The corresponding $\hat{P}_{nad}$ is plotted in Fig. 4(c). Again the differences are small, and there is good quantitative agreement. The maximum error is 0.172.

Equation (18) can also be applied to infinite-time pulses. The approximate P_{nad} obtained from Eq. (18) for the Demkov-Kunike model is plotted in Fig. 3(c). Once again they agree quantitatively with the exact form, Eq. (7), and its contour plot in Fig. 3(b). The maximum error is 0.168.

From Eq. (18) we can derive the asymptotic form of $\hat{P}_{nad}$ in the adiabatic limit,
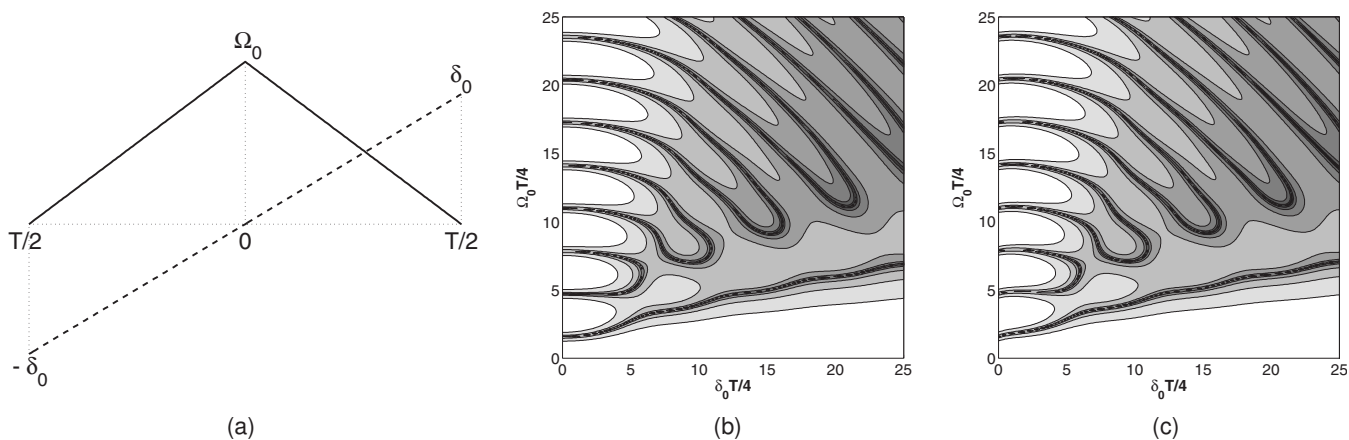
FIG. 4. Contour map of P_{nad} for triangular pulses. (a) The profiles of the pulse detuning and Rabi frequency. (b) The contour curves of $P_{nad}=0.1, 0.01, \ldots$. The darkest regions represent zeros of P_{nad}. (c) The contour plot of the approximate P_{nad}.

$$
\begin{aligned}
\hat{P}_{nad} &= \sin^2\left|\int_0^{T/2} dt\, \dot{\theta}(t)e^{is(t)}\right| \cos^2\left(\arg\int_0^{T/2} dt\, \dot{\theta}(t)e^{is(t)}\right) \\
&\doteq \left|\int_0^{T/2} dt\, \dot{\theta}(t)e^{is(t)}\right|^2 \cos^2\left(\arg\int_0^{T/2} dt\, \dot{\theta}(t)e^{is(t)}\right) \\
&= \left|\mathrm{Re}\int_0^{T/2} dt\, \dot{\theta}(t)e^{is(t)}\right|^2 \doteq \left|\mathrm{Re}\left.\frac{\dot{\theta}(t)e^{is(t)}}{i\Omega'(t)}\right|_0^{T/2}\right|^2 \\
&= \left(\frac{\delta_0^2}{\dot{\Omega}\left(\frac{T}{2}\right)}\right)^{-2} \sin^2\left(\int_0^{T/2}\Omega'(t)dt\right).
\end{aligned}
\tag{20}
$$

Since $\hat{P}_{nad}$ is obtained by perturbation calculation in the rotating adiabatic frame, its asymptotic form in the adiabatic limit is the same as that of the exact P_{nad}, which is given in Eq. (5).

IV. CONCLUSION

By applying unitary first order perturbation in the rotating adiabatic frame, we have derived an approximate formula for the nonadiabatic transition probability P_{nad} for the finite-time

ARP process in the entire parameter space of pulse intensity and detuning. We showed that P_{nad} for finite-time pulses and infinite-time pulses of similar profile has characteristically different distribution in the parameter space. For finite-time pulses, the map of P_{nad} in the pulse parameter space is divided into oscillatory and nonoscillatory regions. The Landau-Zener formula only applies in the nonoscillatory region. In the oscillatory region, the oscillation amplitude and the phase of P_{nad} have different asymptotic forms depending on the region in the parameter space.

The map of P_{nad} in the pulse parameter space provides the critical guidance in the selection of optimal parameters to achieve large optical force using the ARP scheme [2]. The failure of the Landau-Zener formula in the oscillatory region necessitates an approach that is appropriate for finite-time pulses. The agreement between the exact P_{nad} and the approximate formula $\hat{P}_{nad}$ obtained here has proven that the unitary first order perturbation in the rotating adiabatic frame is a successful approach.

[1] T. Lu, X. Miao, and H. Metcalf, Phys. Rev. A **71**, 061405(R) (2005).

[2] X. Miao, E. Wertz, M. G. Cohen, and H. Metcalf, Phys. Rev. A **75**, 011402(R) (2007).

[3] G. Demeter, G. P. Djotyan, Zs. Sörlei, and J. S. Bakos, Phys. Rev. A **74**, 013401 (2006).

[4] L. Allen and J. H. Eberly, *Optical Resonance and Two-Level Atoms* (Dover, New York, 1987).

[5] L. P. Yatsenko, S. Guérin, and H. R. Jauslin, Phys. Rev. A **65**, 043407 (2002).

[6] L. Landau, Phys. Z. Sowjetunion **2**, 46 (1932); C. Zener, Proc. R. Soc. London, Ser. A **137**, 696 (1932).

[7] Yu. N. Demkov and M. Kunike, Vestn. Leningr. Univ., Ser. 4: Fiz., Khim. **16**, 39 (1969).

[8] J. P. Davis and P. Pechukas, J. Chem. Phys. **64**, 3129 (1976).

[9] J. R. Rubbmark, M. M. Kash, M. G. Littman, and D. Kleppner, Phys. Rev. A **23**, 3107 (1981).

[10] K.-A. Suominen and B. M. Garraway, Phys. Rev. A **45**, 374 (1992).

[11] D. Sawicki and J. H. Eberly, Opt. Express **4**, 217 (1999).

[12] C. Cohen-Tannoudji, B. Diu, and F. Laloë, *Quantum Mechanics* (Wiley, New York, 1977).

[13] A. R. P. Rau, Phys. Rev. Lett. **81**, 4785 (1998).

[14] J. J. Sakurai, *Modern Quantum Mechanics* (Addison-Wesley, New York, 1994), Sec. 5.6.